Synthesis and Surface Engineering of Composite Anodes by Coating Thin-Layer Silicon on Carbon Cloth for Lithium Storage with High Stability and Performance

doi: https://doi.org/10.1021/acsaem.1c01049

Syntheses and surface engineering of composite anodes by coating thin-layer silicon on carbon cloth for lithium storage with high stability and performance

Hongbin Liu [†], Xianhe Meng[‡], Yun Chen[†], Yue Zhao[†], Xiaolin Guo[‡], and Tingli Ma[*†‡]*

[†]Graduate School of Life Science and Systems Engineering, Kyushu Institute of Technology, Wakamatsu, Kitakyushu, Fukuoka 808-0196, Japan

[‡]College of Materials and Chemistry, China Jiliang University, Hangzhou 310018, PR China

ABSTRACT

Silicon-flexible carbon composites can achieve binder-free and solve the problem of silicon expansion during cycles. The effective loading and dispersion of silicon onto carbon play an important role in improving the performance of anode materials. Herein, surface engineering of the hole-opening process was successfully achieved before the deposition of silicon. This resulted in fine holes on the carbon cloth, increasing the specific surface area to provide abundant confined space for dispersing nano-silicon. A composite structure was formed and structurally optimized by depositing an ultra-thin silicon layer in the mesoporous holes of

carbon-fiber cloth (DTSi/CC), improving the conductivity of the material, increasing the migration rate of lithium ions, and inhibiting the volume expansion of the anode material during the cycles. At 100 mA g^{-1}, the fabricated half cells achieved a reversible capacity of 1457 mAh g^{-1}, and retained 70.9% initial capacity after 100 cycles. Even when the current density was increased to 1.0 A g^{-1}, it boasted a capacity of 1037 mAh g^{-1} and had 76.8% capacity retention after 500 cycles. Free of binders and conductive additives, the DTSi/CC composite was directly used as the anode exhibiting superior property with high reversible specific capacity, excellent cyclic performance, and good rate capability. This study provides a straightforward, effective route to obtain high-performance silicon-based anode materials for lithium-ion batteries.

KEYWORDS: Surface engineering, Energy, Thin Silicon, LIB anode, Ultra-Stable

INTRODUCTION

Against the backdrop of climate change and dwindling fossil fuel resources, electronic device is becoming more and more important. Lithium-ion batteries, widely used in electronic equipment, electric vehicles, and energy storage, have increasingly higher requirements for energy density, electrochemical cycling, and safety performance. [1-3] However, due to the specific capacity of conventional cathode and anode active materials, it is difficult for current generations of commercial batteries to meet the demand for higher energy density. Therefore, as an important component of lithium-ion batteries, the development and research of new high capacity and rate lithium storage anode materials have extremely research value and widespread application prospects.[4-6] With the abundance and low cost of raw materials and higher theoretical specific capacity of 4200 mAh g^{-1}, the silicon materials have signified a great increase compared to conventional commercial anode materials such as graphite (372 mAh g^{-1}).[7] Silicon materials are

thus considered to be the most promising alternative to graphite for the next-generation of LIBs anodes.[8, 9]

The biggest drawback of silicon-based negative electrodes is that they cannot effectively curb the volume expansion resulting from the charge and discharge process.[10-13] The volume expansion rate of the crystal lattice after charge and discharge is as high as 300%. With the resulting stress unable to be effectively released, the anode material cracks and pulverizes, thereby losing electrical contact with the current collector.[14-17] Furthermore, the SEI film on the surface of the anode material is destroyed, with the constantly regenerating electrolyte film consuming a large amount of electrolytes and causing more side reactions, which ultimately leads to a linear decline of electrochemical performance.[18-20] In addition, the intrinsic conductivity of silicon materials is very low, resulting in a slow electron conduction rate and a poor rate performance of the anode.[21, 22] Evidently, there are still a long way for the application of silicon anode materials.

Due to the above issues, researchers mainly focus on suppressing the volume change and improving the conductivity of the materials, and many solutions have been proposed. First of all, nanometerization of silicon can increase the specific surface area. This can shorten the diffusion channel distance, increase the active sites of reaction, increase the diffusion rate of ions and the conductivity of electrons, and enhance the structural stability of the material. Nano silicon can thus reduce the absolute volume expansion of the anode material and improve stability performance of LIBs. Specifically, there are nanoparticles, nanowires, and nanotubes, etc.[23-27] Next, silicon composite material inhibits the volume expansion, prevents the agglomeration and extrusion of particles, reduces the surface activity, maintains a stable SEI film, and prevents the electrolyte from being consumed continuously. Furthermore, the composite material can greatly

improve the electrical conductivity of the material, adapt to the volume expansion, and improve the cycling performance.[28-31] Thirdly, the silicon-oxygen compound material can form reversible active nano-silicon through the first lithium intercalation reaction, which is evenly distributed among the inert matrix. Although the irreversible component will reduce the initial coulombic efficiency, it can be used as a medium to buffer the active silicon particles in the volume expansion during the de-intercalation and to effectively prevent the agglomeration of nano silicon, showing good electrochemical performance.[32-35]

Constructing a thin silicon layer material is a particularly effective way to enhance the stability of silicon anode materials. The mechanical property of thin-film silicon composite material has been greatly improved.[36, 37] The thin-layer structure can effectively release the internal stress resulting from volume expansion. The direct, close contact between the thin-layer film and the current collector ensures good conductivity, increasing the diffusion efficiency of lithium ion and electrons between the thin layers of silicon. This improves the stability of the battery and raises the initial coulombic efficiency.[38, 39] In this research, we use carbon fiber with good stability and conductivity as the substrate, and create holes on the surface that provides space. Then a thin layer of silicon is deposited, resulting in a kind of sinking silicon-based-carbon composite (DTSi/CC). For DTSi/CC anode material, the thin silicon layer is effectively dispersed and deposited in the manufactured cavity. Because the thin layers are separated by the carbon medium, mutual extrusion caused by the expansion of silicon during the cycling process is reduced. In addition, the porous carbon fiber used as the substrate exhibits good conductivity and flexibility. When combined with silicon, it can be used as a conductive agent, current collector, and without binder. As we expected, when the material is used as anode directly, the stability of silicon anode is greatly improved, showing excellent electrochemical performance. A reversible

capacity of 1037 mAh g^{-1} was achieved at 1.0 A g^{-1}, and 76.8% of the original capacity was retained without obvious decline after 500 cycles.

EXPERIMENTAL SECTION

Materials

The analytical grade of reagents in synthesis were used as purchased and used directly without other processing. Ammonia (28~30%), tetraethyl Orthosilicate (TEOS) (≥95%), Magnesium Powder (≥99%), hexamethylenetetramine (≥99%), Hydrochloric acid (36.5~40%), Nickel nitrate hexahydrate (≥99%) were purchased from Wako Pure Chemical Corporation.

Part of the experimental process refers to the literature.[40]

Preparation of porous carbon cloth (PCC)

4 mmol hexamethylenete-tramine and 2 mmol nickel nitrate hexahydrate were added to 20 mL of deionized water to form light green mixed solution. After 30 minutes of full dissolution, we transferred the solution to a 50 ml polytetrafluoroethylene autoclave. Then the pretreated CC (refer to the literature for the preparation process [27]) was immersed and transferred to an oven at 95 °C for 6h. After cooling, washing, and drying overnight, the sample light green nanoflakes array NiOOH coated carbon cloth (NiOOH/CC) was obtained. Following this, NiOOH/CC was annealed at 700°C, 800°C, and 900 °C in argon for three hours (the samples were named PCC-700, PCC-800 and PCC-900, respectively), then immersing in 2 M hydrochloric acid for 2 days to remove impurities. Finally, all these porous carbon clothes were washed several times and then dried overnight.

Depositing nano thin layer SiO_2 on porous CC ($DSiO_2$/CC)

50ml water and 50ml ethanol was mixed through stirring, then dropped into 10 ml ammonia solution in 5min. After 30 min, added 8 ml of tetraethyl orthosilicate in 10min. Followed by putting obtained porous CC into the mixed solution and oscillating for 12 h. Next, the porous carbon fibers loaded the SiO_2 sample was separated, washed several times, and dried overnight at 70 °C to obtain the $SSiO_2$/CC sample.

Synthesis of DTSi/CC

The silicon thin layer was obtained by mixing the $DSiO_2$/CC sample with magnesium powder through reduction. Specifically, $DTSiO_2$/CC sample was mixed with Mg powder in a one-to-one ratio; then the reactants were transferred into a tube furnace and heated under argon atmosphere for 6 hours at 650 °C. After cooling the sample to room temperature, immersing in hydrochloric acid (0.5 M) for 3 hours. Next, the depositing thin layer silicon on the carbon cloth sample was separated, washed several times, and dried overnight.

Synthesis of pure Silicon on CC (p-Si/CC)

A pure silicon sample was prepared for comparison. The clean carbon cloth was transferred into the tube furnace under argon atmosphere and heated for 6 hour at 650 °C. Pure nano silicon powder was used to prepare the material slurry with the binder of polyvinylidene fluoride (weight ratio = 9:1). The carbon cloth was coated with the mixed slurry, dried for 2h at 70 °C, and then dried further for 6 h at 110 °C under vacuum to obtain the p-Si/CC sample.

RESULTS AND DISSCUSSION

Structure and morphology of the designed silicon/carbon composite

The synthesis strategy can be divided into several steps, as shown in scheme 1. First, a layer of NiOOH thin nanosheets was applied on the surface of the carbon cloth. After high-temperature

air isolation treatment, the generated NiOOH reacts with the smooth surface of the carbon cloth to generate Ni elementary substance, which is condensed into a block and embedded into the carbon fibers. After acid washing, holes are formed on the surface of the carbon fibers, increasing the specific surface area of the carbon cloth, and providing space for the subsequent deposition of silicon. Hydrolyzed silane was used to introduce a silicon source onto the surface of the carbon fiber with the pores. Finally, magnesium reduction was used to obtain the final material. The detailed synthesis process is described in the experimental section.

Scheme 1. Synthetic strategy process of DTSi/CC through the surface engineering treatment carbon cloth and depositng thin silicon.

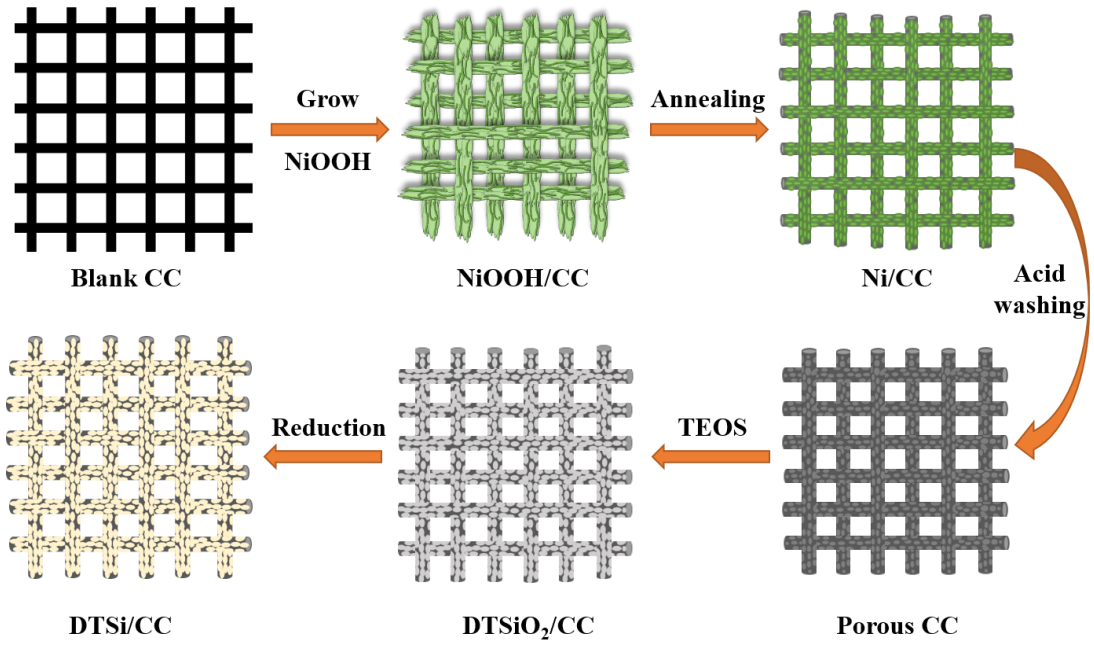

The material changes that occurred through the whole process of the experiment can be seen from the SEM images in Figure 1 and Figure S1. From the initial synthesis, carbon fiber material with smooth surfaces and uniform dimensions were used (Figure 1a). After hydrothermal growth,

a uniform layer of NiOOH nanoflake grows on the carbon fiber. After calcination, the carbon on the carbon cloth reacts with the attached NiOOH to form Ni metal, which is embedded in the carbon fibers (Figure 1c, S1a). The resulting carbon fiber was immersed in an acid solution and the Ni metal embedded in it was removed to obtain the porous carbon fiber structure (Figure 1d). The size of the hole is about 500 nm after annealing at 800℃. The pore diameter synthesized at low temperature 700℃ is about 200 nm, with a sparser pore density (Figure S1b). The pore size of the carbon cloth synthesized at 900℃ is about 1 micron, with some of the carbon fibers visibly damaged (Figure S1c). Hydrolyzing and depositing a layer of silicon oxide on the carbon cloth and then reducing it with magnesium resulted in a material that is trapped in a thin layer of silicon on the porous carbon cloth. A layer of nano silicon was uniformly attached to the surface of the otherwise smooth holes in the carbon cloth (Figure 1e, f).

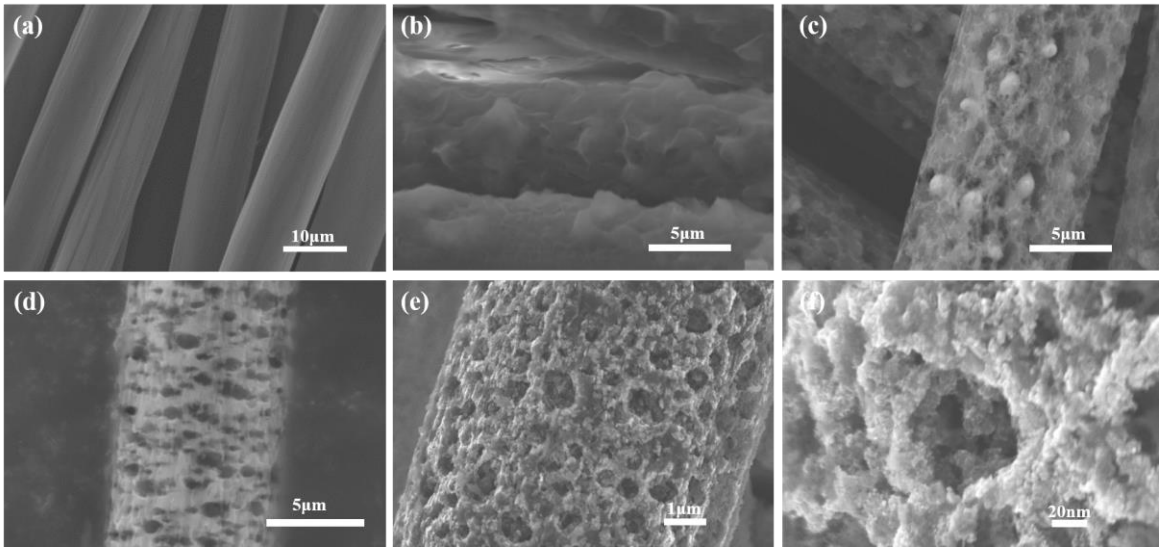

Figure 1. (a) SEM image of the blank carbon cloth, (b) coated with a NiOOH layer, (c) after annealing at 800 ℃, (d) PCC-800, and (e, f) DTSi/CC-800.

TEM results reveal further details of the DTSi/CC-800 material. From Figure 2 (a, b), a silicon layer on the surface of the carbon cloth with a certain porous structure can be seen. EDS (Energy

Dispersive Spectrometer) mapping was used to analyze the element distribution of Si materials (Figure 2c-e). The diagram shows that the carbon element is tightly surrounded by silicon.

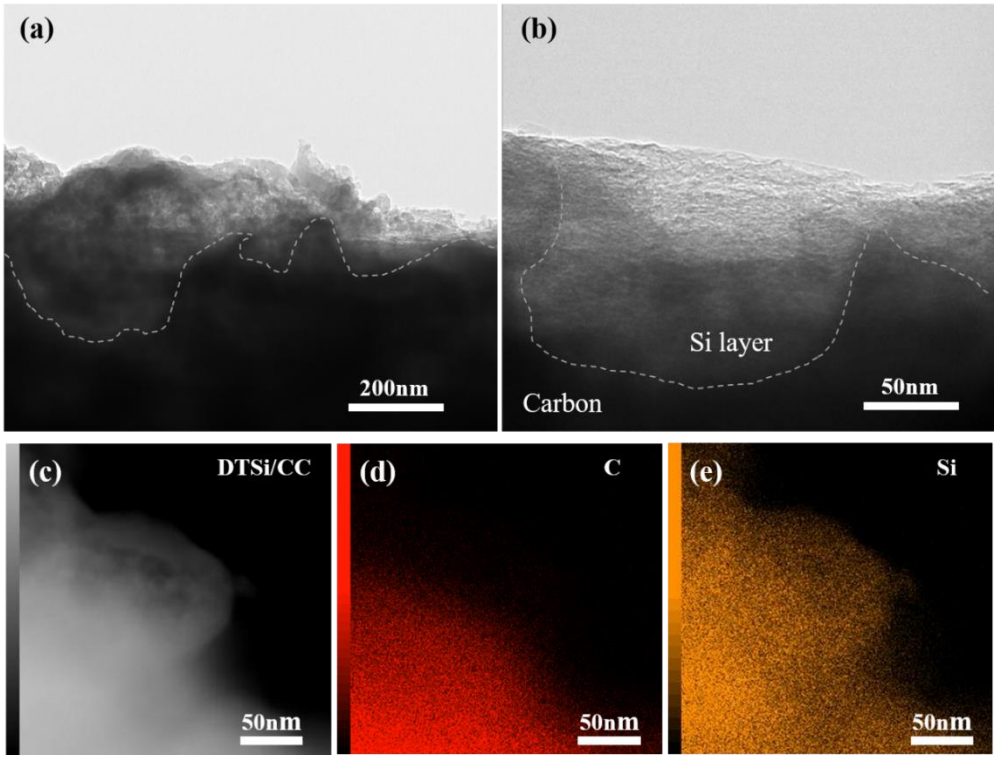

Figure 2. (a, b) TEM and HRTEM images of the DTSi/CC-800. (c-e) Elemental mapping images of the DTSi/CC-800.

XRD diffraction patterns were used to analyze the phase composition of the DTSi/CC-800 sample (Figure 3a). In addition to the two diffuse peaks which can be attributed to the amorphous carbon substrate at 25.4° and 43.3°, the characteristic peaks at 28.5°, 47.1°, 56.2°, 69.1° and 76.6° attributed to (111), (220), (311), (400) and (331) lattice planes, respectively, belong to the pure silicon phase. Apparently, a pure crystalline silicon layer has formed on the porous carbon cloth substrate. To further elaborate the crystallinity of silicon in the porous carbon cloth, a Raman spectrum was test (Fig. 3b). The peak at 510.1 cm^{-1} shows the transverse

optical mode of single crystal silicon. And the two weak peaks at 290.1 cm^{-1} and 922.0 cm^{-1}, which can be ascribed to the first and second-order transverse optical mode of amorphous silicon, respectively.[41] This again demonstrates that the silicon sinking on the porous carbon fiber exhibits good crystallinity, with only a small amount of amorphous silicon mixed in the DTSi/CC-800.

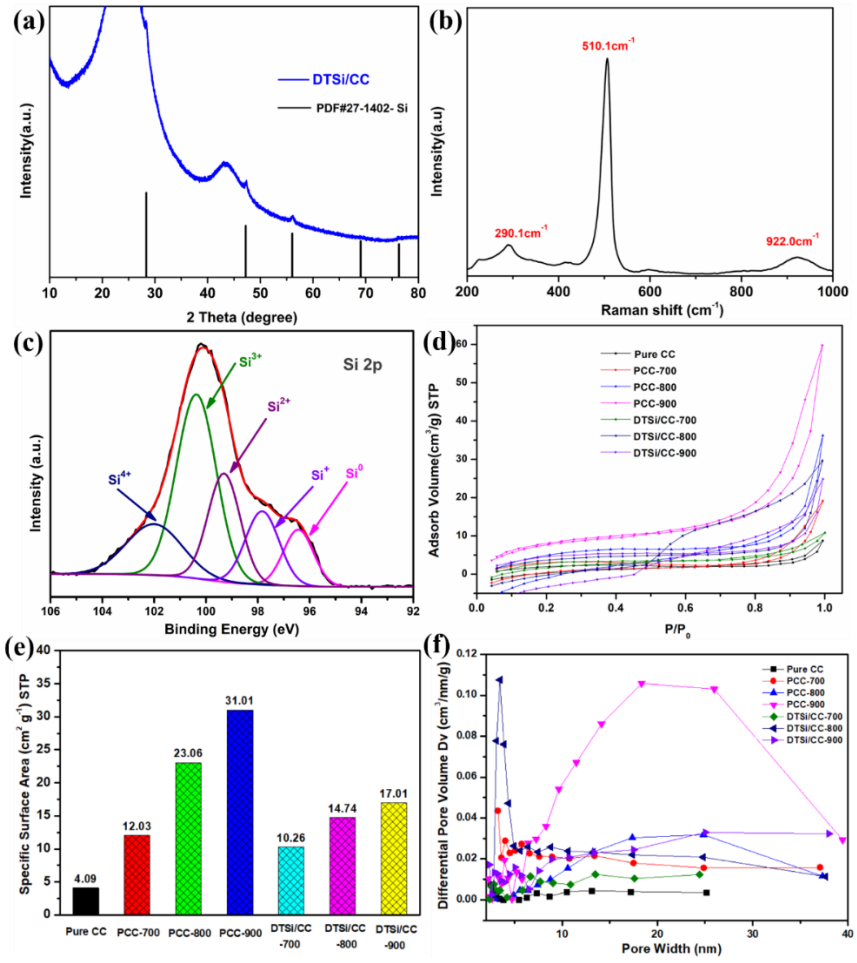

Figure 3. (a) XRD patterns, (b) Raman spectra, (c) XPS spectra of the Si 2p of DTSi/CC-800, (d) and nitrogen adsorption−desorption isotherm of the DTSi/CC-800 and other comparison samples. (e) Calculated specific surface area of pure CC, PCC-800, DTSi/CC-800, and others samples, and (f) the BJH pore size distribution of the DTSi/CC-800 and other comparison samples.

Figure 3c shows the XPS diagram of the material, which is used to explain the valence state of the deposited thin silicon on the porous carbon fiber. The peaks of Si 2p could be divided into five individual peaks at 102.0, 100.4, 99.4, 97.8, and 96.4 eV, which can be ascribed to Si^{4+}, Si^{3+}, Si^{2+}, Si^{+}, and Si^{0}, respectively. The tetravalent silicon is mainly belong to the impurity SiO_2 in the final product, and the remaining valence state indicates that the existence of SiO_x. This will cause some irreversible capacity loss during the battery cycles.[42] The presence of polyvalent states of silicon indicates that a small portion of the DTSi/CC-800 surface is oxidized due to crystalline silicon in contact with air.[43] The O 1S peak of the DTSi/CC-800 sample appearing (Figure S2) corroborate this finding.

We also test nitrogen adsorption and desorption to describe the synthetic distinctive porous structure of DTSi/CC material. To confirm the reliability of the surface engineering holes making, we prepared parallel samples at different temperatures for comparison (PCC-700, PCC-800, PCC-900). The Brunauer-Emmett-Teller (BET) model was used to calculate the specific surface areas of the various materials. Figure 3d illustrates the N_2-adsorption isotherms of the DTSi/CC sample and the products during the experiment, as well as other comparative samples. Excitingly, the surface engineering hole making increases the specific surface area of the carbon fiber from 4.09 $m^2 g^{-1}$ to 31.01 $m^2 g^{-1}$ (Figure 3e) without breaking the integrity. Also, when silicon is deposited in the pores, instead of blocking them up completely, the specific surface area of the material increases exponentially (10.26 $m^2 g^{-1}$ DTSi/CC-700, 14.74 $m^2 g^{-1}$ DTSi/CC-800, 17.01 $m^2 g^{-1}$ DTSi/CC-900). Given this significant increase in specific surface area, we attached a larger amount of thin layer of silicon to encourage rapid diffusion of lithium ions through the material, hoping to improving stability and storage capacity. Figure 3f illustrates the

pore disaster distribution of those samples. Evidently, the pore size distribution of our final synthesized material is more varied, ranging from 3nm to 40nm, with sufficient mesopores.

Electrochemical performances

The electrochemical property of the DTSi/CC samples was verified by the assembly of coin cells, which used lithium plates for the counter electrodes. The electrochemical cycling performance at 100 mA g^{-1} was investigated first. In Figure 4a and b, the initial charging and discharging capacities of the DTSi/CC-800 were approximately 2206.6 mAh g^{-1} and 1590.5 mAh g^{-1}, and the initial coulombic efficiency was 72.1%. The formation of a stable solid electrolyte interphase (SEI) film in the initial stage was the main reason behind the irreversible capacity. It is noteworthy that after a long cycle, in addition to the capacity loss by SEI at the first cycle, the battery assembled with DTSi/CC-800 material still exhibited a good capacity retention rate. After 100 cycles, the battery could still maintain 94.22% of the original reversible cycle and the coulomb efficiency in the cycles could be kept above 99.5%. This indicates that the material synthesized by surface engineering strategy to form porous carbon fiber with deposited silicon can effectively improve the stability of the silicon anode material in lithium-ion batteries. To further explore the effectiveness of the material during cycles, we increased the current density of charge and discharge to 1.0 mA g^{-1}. In Figure 4e, after 500 cycles, the anode composed of the DTSi/CC-800 displayed outstanding stability and good specific capacity, reaching 1037.8 mAh g^{-1}, maintaining 77.0% of the initial capacity and a coulomb efficiency above 99.5%.

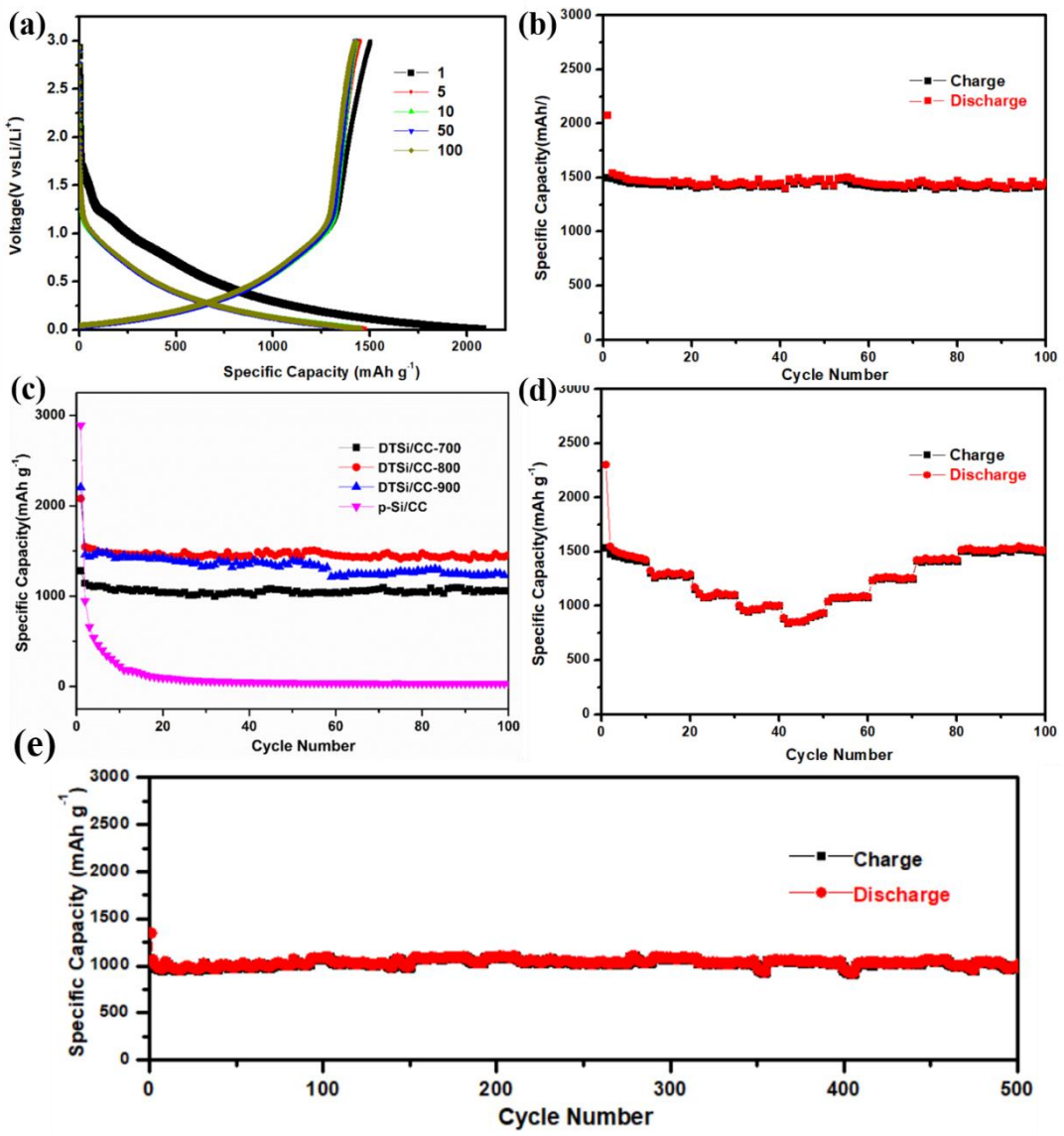

Figure 4. (a) The charge and discharge profiles for the 1st, 5th, 10th, 50th and 100th cycles of DTSi/CC-800 at 100 mA g^{-1}. (b) Cycling performance of DTSi/CC between the range of 0.01-3.0V at 100 mA g^{-1}. (c) Comparison of cycling performance of DTSi/CC-700, DTSi/CC-800, DTSi/CC-900 and pure Si/CC between the range of 0.01-3.0V at 100 mA g^{-1}. (d) Rate capability of DTSi/CC. (e) Cycling performance of DTSi/CC-800 at 1.0 A g^{-1} for 500cycles.

To show the superiority of DTSi/CC-800 materials synthesized by surface engineering strategy proposed here, we compared the materials synthesized at different annealing temperatures, and the silicon powder directly attached to the carbon cloth, as shown in Figure 4c. The three materials synthesized at different temperatures vary in pore size, density and depth of the porous carbon. Compared with the carbon fibers synthesized at 800 ℃, the smaller size of pores on the carbon fibers was synthesized 700 ℃, shallower depth and lower density. The porous carbon fibers synthesized at 900 ℃ have larger and deeper holes. Compared with DTSi/CC-800, the specific capacity of DTSi/CC-700 is significantly lower. It has a discharge specific capacity of 1059.7 mAh g^{-1} after 100 cycles. This is because in the deposition process, due to the low density, shallow depth and small size of the holes in the carbon fiber, the space of the holes to be compressed, and the space provided to adapt to the expansion becomes smaller, which leads to a decrease in performance during the cycles. The initial discharge specific capacity of the DTSi/CC-900 anode material is much higher, up to 2205.1 mAh g^{-1}, but it gradually decreases over time. After 100 cycles were completed, the specific capacity was reduced to 1231.1 mAh g^{-1}, and only 55.8% of the initial discharge specific capacity can be maintained. This is because the holes in the PCC-900 are too large and dense. When the silicon is deposited, it is piled up very densely. In the electrochemical cycles, the expanded silicon is squeezed significantly, which results in declining of capacity. In addition, part of the carbon fiber breaks under the penetration of the high density holes, precipitating falling off of the anode material and worsening electrode stability. The p-Si/CC anode materials with the binder have the highest initial specific capacity of 2890.5 mAh g^{-1}, but they maintain 458.5 mAh g^{-1} at 5^{th} cycle, with a disappointing decline rate of 84.1%. The specific capacity is mere 41.0 mAh g^{-1} at 50^{th} cycle, and the decline rate is 98.1%. Evidently, the stability of silicon anode material can be significantly improved by the

surface engineering strategy of forming porous carbon fiber with a thin layer of silicon. Yet, when the porous carbon fiber substrate of DTSi/CC material is synthesized, the density and size of the holes formed should be moderate so as to ensure that the materials displays excellent and stable performance.

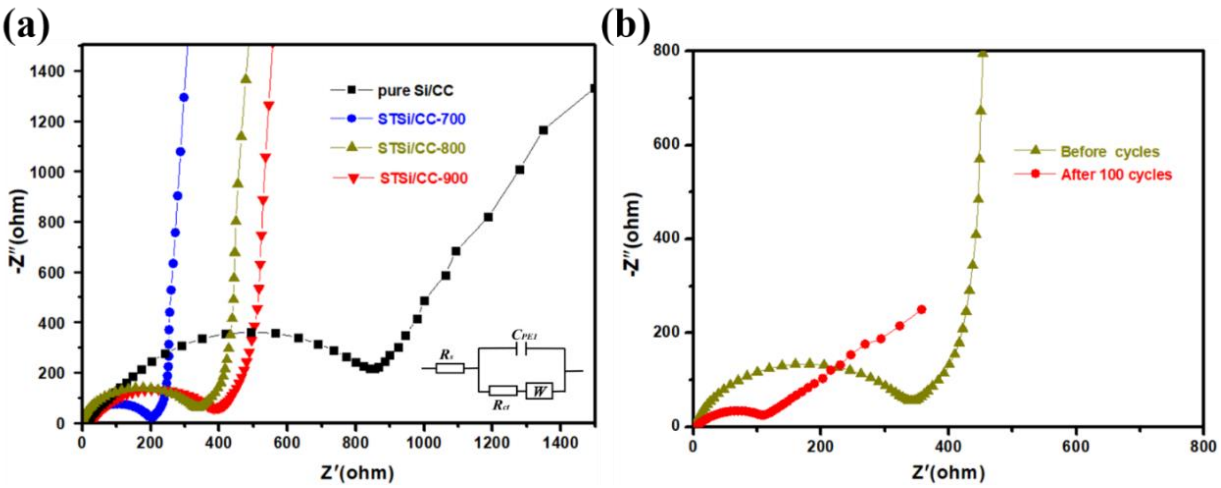

Figure 5. (a) The EIS of DTSi/CC-700, DTSi/CC-800, DTSi/CC-800 and pure Si/CC anode. The small graph insert in the Fig. is the equivalent circuit. (b) The EIS of DTSi/CC-800 after 100 cycles.

The rate specific capacities of the DTSi/CC anode materials were also tested (Figure 4d). At the different current densities of 0.1 A g^{-1}, 0.2 mA g^{-1}, 0.5 mA g^{-1}, 1.0 A g^{-1}, and 2.0 A g^{-1}, the average discharge specific capacity of DTSi/CC-800 anode material are 1474.7 mAh g^{-1}, 1296.7 mAh g^{-1}, 1110.2 mAh g^{-1}, 1031.5 mAh g^{-1}, and 883.3 mAh g^{-1}, respectively. When charge-discharge current reverts to 0.1 A g^{-1} again, the discharge specific capacity of the DTSi/CC-800 material restored to 1518.7 mAh g^{-1}. This indicates that the DTSi/CC-800 anode material

exhibits excellent recovery and reversible electrochemical cycling performance. This is further demonstrated by the ultra-high stability of 500 cycles (Figure 4e).

The electrical conductivity of cells assembled from different materials was analyzed by electrochemical impedance spectroscopy (EIS) (Figure 5a). The curve is mainly composed of a semicircle and a straight line. The former is in the high frequency region formed by the charge transfer resistance (Rct). The latter is in the low frequency region formed by the diffusion and transfer of lithium ions in the electrolyte represented by the Warburg impedance.[44] Among DTSi/CC-700, DTSi/CC-800, DTSi/CC-900 and p-Si/CC, the Rct of DTSi/CC-700 is the smallest, followed by DTSi/CC-800, with p-Si/CC being the worst. This indicates that the charge transfer resistance increases as more silicon is loaded on the porous carbon substrate, causing a decrease of electrical conductivity. Compared with the p-Si/CC anode material, the Rct of the other three materials obtained by constructing porous carbon fiber using surface engineering strategy and depositing a thin layer of silicon is much lower. The EIS of the DTSi/CC-800 anode after 100 cycles is also shown in Figure 5b. Evidently, after cycles, the Rct of the DTSi/CC-800 electrode was much smaller than at the start, displaying its enhanced electrochemical nature. The reaction diagram in Figure 6a is used to explain this. When the carbon fibers are completely covered by the silicon layer, the conductivity is reduced, and the silicon layers are not significantly isolated. Thus, during the cycles, lithium is inserted to form an alloy silicon layer. It will be squeezed, and since the stress cannot be effectively released, the material begins to exfoliate. The silicon layer of the DTSi/CC material can be well dispersed in the porous structure, and the space formed can effectively relieve mechanical pressure (Figure 6b). This shows that the silicon anode materials synthesized in proposed way effectively improves the electrical conductivity, greatly enhance the stability in lithiation-delithiation cycles.

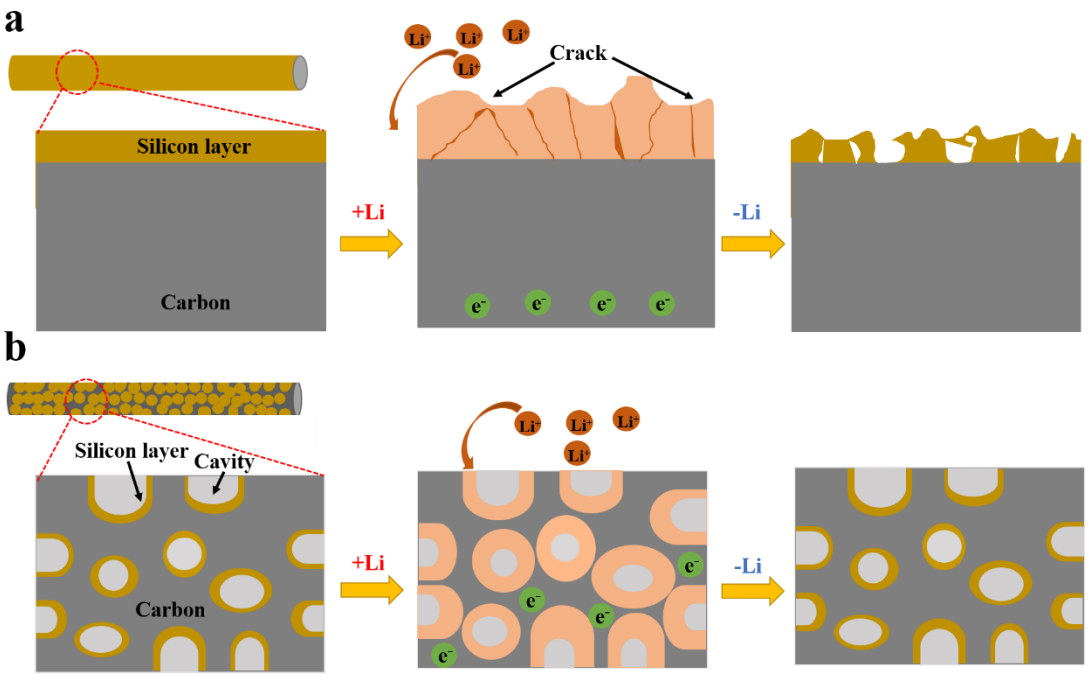

Figure 6. Schematic diagram of surface engineering synthetic DTSi/CC. (a) Sample coating pure silicon and (b) DTSi/CC.

CONCLUSIONS

By deploying a surface engineering strategy, a carbon-fiber substrate with sufficient mesoporous in a certain range was successfully constructed, and thin layer of silicon ware deposited on it. Adjusting the synthesis at different temperatures, we selected the DTSi/CC-800 composite as binder-free LIBs anode with the best electrochemical performance. After 500 cycles of cycles, it still exhibits a reversible capacity of 1037.8 mAh g^{-1} at 1000 mA g^{-1}, and the decay rate being less than one quarter. The mesopores of DTSi/CC-800 can compact closely with the nano silicon due to the confinement effect, forming a stable SEI film that facilitates effective electron and lithium ions transport. This structure, moreover, has plenty of buffer space to relieve the stress of the extrusion of silicon materials, effectively inhibiting the volume expansion of the

anode materials. This is the main reason for why battery is able to maintain its super-stable electrochemical performance. This work provides a rational surface-design strategy for stable silicon/carbon anodes with improved performance for next-generation LIBs.

ASSOCIATED CONTENT

Supporting Information.

Materials characterization; Measurement of the electrochemical properties; SEM images during synthesis; full XPS Spectrum; electrochemical performance of cycling.

AUTHOR INFORMATION

Corresponding Author

*E-mail: tinglima@life.kyutech.ac.jp (T. M.), ORCID: 0000-0002-3310-459X.

*E-mail: mengxhe@cjlu.edu.cn (X. M.), 0000-0002-9856-2268.

Notes

The authors declare no competing financial interest.

ACKNOWLEDGMENT

This work was supported by "Nanotechnology Platform Program" of the Ministry of Education, Culture, Sports, Science and Technology (MEXT), Japan, Grant Number JPMXP09F-19-FA-0029 and KAGENHI Grant-in-Aid for Scientific Research(B), No.19H02818, Iwatani Naoji Foundation, and the National Natural Science Foundation of China (Grant No. 51772039 and 51972293).

REFERENCES

(1) Harper, G.; Sommerville, R.; Kendrick, E.; Driscoll, L.; Slater, P.; Stolkin, R.; Walton, A.; Christensen, P.; Heidrich, O.; Lambert, S.; Abbott, A.; Ryder, K.; Gaines, L.; Anderson, P., Recycling lithium-ion batteries from electric vehicles. *Nature* **2019**, 575, 75-86.

(2) Zheng, M.; Tang, H.; Hu, Q.; Zheng, S.; Li, L.; Xu, J.; Pang, H., Tungsten-Based Materials for Lithium-Ion Batteries. *Advanced Functional Materials* **2018**, 28, 1707500.

(3) Tarascon, J. M. & Armand, M.; Issues and challenges facing rechargeable lithium batteries. *Nature*, **2001**, 414, 359–367.

(4) Pomerantseva, E.; Bonaccorso, F.; Feng, X.; Cui, Y.; Gogotsi, Y., Energy storage: The future enabled by nanomaterials. *Science* **2019**, 366, 969.

(5) Sarang, K. T.; Zhao, X.; Holta,D.; Radovic, M.; Green, M. J.; Oh, E. S.; and Lutkenhaus, J. L.; Minimizing Two-Dimensional Ti3C2Tx MXene Nanosheet Loading in Carbon-free Silicon Anodes. *Nanoscale*, **2020**, 12, 20699-20709

(6) Zhang, L.; Wang, C.; Dou, Y.; Cheng, N.; Cui, D.; Du, Y.; Liu, P.; Al-Mamun, M.; Zhang, S.; Zhao, H., A Yolk-Shell Structured Silicon Anode with Superior Conductivity and High Tap Density for Full Lithium-Ion Batteries. *Angewandte Chemie* **2019**, 58, 8824-8828.

(7) Luo, C.; Du, L.; Wu, W.; Xu, H.; Zhang, G.; Li, S.; Wang, C.; Lu, Z.; Deng, Y., Novel Lignin-Derived Water-Soluble Binder for Micro Silicon Anode in Lithium-Ion Batteries. *ACS Sustainable Chemistry & Engineering* **2018**, 6, 12621-12629.

(8) Kwon, T. W.; Choi, J. W.; Coskun, A., The emerging era of supramolecular polymeric binders in silicon anodes. *Chemical Society reviews* **2018**, 47, 2145-2164.

(9) Cangaz, S.; Hippauf, F.; Reuter, F. S.; Doerfler, S.; Abendroth, T.; Althues, H.; Kaskel, S., Enabling High‐Energy Solid‐State Batteries with Stable Anode Interphase by the Use of Columnar Silicon Anodes. *Advanced Energy Materials* **2020**, 10, 2001320.

(10) Chen, X.; Gerasopoulos, K.; Guo, J.; Brown, A.; Wang, C.; Ghodssi, R.; and Culver, J. N.; Virus-Enabled Silicon Anode for Lithium-Ion Batteries. *ACS Nano*, **2010**, 4, 5366–5372.

(11) Ohara, S.; Suzuki, J.; Sekine, K.; Takamura, T., A thin film silicon anode for Li-ion batteries having a very large specific capacity and long cycle life. *Journal of Power Sources* **2004**, 136, 303-306.

(12) Guo, J.; Wang, C., A polymer scaffold binder structure for high capacity silicon anode of lithium-ion battery. *Chemical communications* **2010**, 46, 1428-30.

(13) Chockla, A. M.; Harris, J. T.; Akhavan, V. A.; Bogart, T. D.; Holmberg, V. C.; Steinhagen, C.; Mullins, C. B.; Stevenson, K. J.; Korgel, B. A., Silicon nanowire fabric as a lithium ion battery electrode material. *Journal of the American Chemical Society* **2011**, 133, 20914-21.

(14) Franco Gonzalez, A.; Yang, N.-H.; Liu, R.-S., Silicon Anode Design for Lithium-Ion Batteries: Progress and Perspectives. *The Journal of Physical Chemistry C* **2017**, 121, 27775-27787.

(15) Liu, Z.; Yu, Q.; Zhao, Y.; He, R.; Xu, M.; Feng, S.; Li, S.; Zhou, L.; Mai, L., Silicon oxides: a promising family of anode materials for lithium-ion batteries. *Chemical Society reviews* **2019**, 48, 285-309.

(16) Ge, M.; Rong, J.; Fang, X.; Zhou, C., Porous doped silicon nanowires for lithium ion battery anode with long cycle life. *Nano letters* **2012**, 12, 2318-23.

(17) Zhao, J.; Liao, L.; Shi, F.; Lei,T.; Chen, G.; Pei, A.; Sun, J.; Yan, K.; Zhou, G.; Xie, J.; Liu, C.; Li, Y.; Liang, Z.; Bao, Z.; and Cui, Y., Surface fluorination of reactive battery anode materials for enhanced stability. *J. Am. Chem. Soc.*, **2017**, 139, 11550–11558.

(18) Zheng, J.; Zheng, H.; Wang, R.; Ben, L.; Lu, W.; Chen, L.; Chen, L.; Li, H., 3D visualization of inhomogeneous multi-layered structure and Young's modulus of the solid electrolyte interphase (SEI) on silicon anodes for lithium ion batteries. *Physical chemistry chemical physics* **2014**, 16, 13229-38.

(19) Yoon, T.; Milien, M. S.; Parimalam, B. S.; Lucht, B. L., Thermal Decomposition of the Solid Electrolyte Interphase (SEI) on Silicon Electrodes for Lithium Ion Batteries. *Chemistry of Materials* **2017**, 29, 3237-3245.

(20) Jin, Y.; Li, S.; Kushima, A.; Zheng, X.; Sun, Y.; Xie, J.; Sun, J.; Xue, W.; Zhou, G.; Wu, J.; Shi, F.; Zhang, R.; Zhu, Z.; So, K.; Cui, Y.; Li, J., Self-healing SEI enables full-cell cycling of a silicon-majority anode with a coulombic efficiency exceeding 99.9%. *Energy & Environmental Science* **2017**, 10, 580-592.

(21) Liu, D.; Zhao, Y.; Tan, R.; Tian, L.-L.; Liu, Y.; Chen, H.; Pan, F., Novel conductive binder for high-performance silicon anodes in lithium ion batteries. *Nano Energy* **2017**, 36, 206-212.

(22) Bonaccorso, F.; Colombo, L.; Yu, G.; Stoller, M.; Tozzini, V.; Ferrari, A. C.; Ruoff, R. S.; Pellegrini, V., 2D materials. Graphene, related two-dimensional crystals, and hybrid systems for energy conversion and storage. *Science* **2015**, 347, 1246501.

(23) Chen, S.; Shen, L.; van Aken, P. A.; Maier, J.; Yu, Y., Dual-Functionalized Double Carbon Shells Coated Silicon Nanoparticles for High Performance Lithium-Ion Batteries. *Advanced materials* **2017**, 29, 1605650.

(24) Sun, H.; Xin, G.; Hu, T.; Yu, M.; Shao, D.; Sun, X.; Lian, J., High-rate lithiation-induced reactivation of mesoporous hollow spheres for long-lived lithium-ion batteries. *Nature communications* **2014**, 5, 4526.

(25) Liang, J.; Li, X.; Zhu, Y.; Guo, C.; Qian, Y., Hydrothermal synthesis of nano-silicon from a silica sol and its use in lithium ion batteries. *Nano Research* **2014**, 8, 1497-1504.

(26) Liu, J.; Kopold, P.; van Aken, P. A.; Maier, J.; Yu, Y., Energy Storage Materials from Nature through Nanotechnology: A Sustainable Route from Reed Plants to a Silicon Anode for Lithium-Ion Batteries. *Angewandte Chemie* **2015**, 54, 9632-6.

(27) Liu, H.; Chen, Y.; Jiang, B.; Zhao, Y.; Gu, X. and Ma, T., Hollow-Structure Engineering of Silicon-Carbon Anode for Ultra-Stable Lithium-ion Batteries. *Dalton Trans.* **2020**, 49, 5669-5676.

(28) Fuchsbichler, B.; Stangl, C.; Kren, H.; Uhlig, F.; Koller, S., High capacity graphite–silicon composite anode material for lithium-ion batteries. *Journal of Power Sources* **2011**, 196, 2889-2892.

(29) Wang, Z.; Mao, Z.; Lai, L.; Okubo, M.; Song, Y.; Zhou, Y.; Liu, X.; Huang, W., Sub-micron silicon/pyrolyzed carbon@natural graphite self-assembly composite anode material for lithium-ion batteries. *Chemical Engineering Journal* **2017**, 313, 187-196.

(30) Jia, H.; Li, X.; Song, J.; Zhang, X.; Luo, L.; He, Y.; Li, B.; Cai, Y.; Hu, S.; Xiao, X.; Wang, C.; Rosso, K. M.; Yi, R.; Patel, R.; Zhang, J. G., Hierarchical porous silicon structures with extraordinary mechanical strength as high-performance lithium-ion battery anodes. *Nature communications* **2020**, 11, 1474.

(31) Xu, Y.; Zhu, Y.; Wang, C., Mesoporous carbon/silicon composite anodes with enhanced performance for lithium-ion batteries. *J. Mater. Chem. A* **2014**, 2, 9751-9757.

(32) Zhang, Y.; Jiao, Y.; Lu, L.; Wang, L.; Chen, T.; Peng, H., An Ultraflexible Silicon-Oxygen Battery Fiber with High Energy Density. *Angewandte Chemie* **2017**, 56, 13741-13746.

(33) He, W.; Liang, Y.; Tian, H.; Zhang, S.; Meng, Z.; Han, W.-Q., A facile in situ synthesis of nanocrystal-FeSi-embedded Si/SiOx anode for long-cycle-life lithium ion batteries. *Energy Storage Materials* **2017**, 8, 119-126.

(34) Wang, M.; Xia, Y.; Wang, X.; Xiao, Y.; Liu, R.; Wu, Q.; Qiu, B.; Metwalli, E.; Xia, S.; Yao, Y.; Chen, G.; Liu, Y.; Liu, Z.; Meng, J. Q.; Yang, Z.; Sun, L. D.; Yan, C. H.; Muller-Buschbaum, P.; Pan, J.; Cheng, Y. J., Silicon Oxycarbide/Carbon Nanohybrids with Tiny Silicon Oxycarbide Particles Embedded in Free Carbon Matrix Based on Photoactive Dental Methacrylates. *ACS applied materials & interfaces* **2016**, 8, 13982-92.

(35) Zhu, G.; Gu, Y.; Heng, S.; Wang, Y.; Qu, Q.; Zheng, H., Simultaneous growth of SiOx/carbon bilayers on Si nanoparticles for improving cycling stability. *Electrochimical Acta* **2019**, 323, 134840.

(36) Wang, C.; Chui, Y.-S.; Ma, R.; Wong, T.; Ren, J.-G.; Wu, Q.-H.; Chen, X.; Zhang, W., A three-dimensional graphene scaffold supported thin film silicon anode for lithium-ion batteries. *Journal of Materials Chemistry A* **2013**, 1, 10092.

(37) Son, Y.; Ma, J.; Kim, N.; Lee, T.; Lee, Y.; Sung, J.; Choi, S. H.; Nam, G.; Cho, H.; Yoo, Y.; Cho, J., Quantification of Pseudocapacitive Contribution in Nanocage‐Shaped Silicon–Carbon Composite Anode. *Advanced Energy Materials* **2019**, 9, 1803480.

(38) Jiang, C.; Xiang, L.; Miao, S.; Shi, L.; Xie, D.; Yan, J.; Zheng, Z.; Zhang, X.; Tang, Y., Flexible Interface Design for Stress Regulation of a Silicon Anode toward Highly Stable Dual-Ion Batteries. *Advanced materials* **2020**, 32, e1908470.

(39) Fan, Y.; Zhang, Q.; Xiao, Q.; Wang, X.; Huang, K., High performance lithium ion battery anodes based on carbon nanotube–silicon core–shell nanowires with controlled morphology. *Carbon* **2013**, 59, 264-269.

(40) Balogun, M.-S.; Qiu, W.; Lyu, F.; Luo, Y.; Meng, H.; Li, J.; Mai, W.; Mai, L.; Tong, Y., All-flexible lithium ion battery based on thermally-etched porous carbon cloth anode and cathode. *Nano Energy* **2016**, 26, 446-455.

(41) Zhang, L.; Hu, X.; Chen, C.; Guo, H.; Liu, X.; Xu, G.; Zhong, H.; Cheng, S.; Wu, P.; Meng, J.; Huang, Y.; Dou, S.; Liu, H., In Operando Mechanism Analysis on Nanocrystalline Silicon Anode Material for Reversible and Ultrafast Sodium Storage. *Advanced materials* **2017**, 29, 1604708.

(42) Taeseung, Y., Taesoo, B., Chulhyun, K., Younghoon, Na., Soojin, Park. and Kwang. S. Kim., Mesoporous Silicon Hollow Nanocubes Derived from Metal−Organic Framework Template for Advanced Lithium-Ion Battery Anode. *ACS Nano*, **2017**, 11, 4808−4815

(43) BARR, T. L., An XPS study of Si as it occurs in adsorbents, catalysts, and thin films. *Applications of Surface Science*, **1983**, 15, 1-35.

(44) Paloukis, F.; Elmasides, C.; Farmakis, F.; Selinis, P.; Neophytides, S. G.; Georgoulas, N., Electrochemical Impedance Spectroscopy study in micro-grain structured amorphous silicon anodes for lithium-ion batteries. *Journal of Power Sources* **2016**, 331, 285-292.